THE PHOTOCHEMISTRY OF BIOGENIC GASES IN THE EARLY AND PRESENT ATMOSPHERE

JOEL S. LEVINE and TOMMY R. AUGUSTSSON*

Atmospheric Sciences Division, NASA Langley Research Center, Hampton, Virginia 23665, U.S.A.

(Received 21 March, 1985)

1. Introduction

The role of the biosphere in the production and regulation of major (nitrogen (N_2) and oxygen (O_2)) and minor (carbon dioxide (CO_2)) atmospheric gases has been fully appreciated for many years. The realization of the importance of the biosphere as a source of trace atmospheric gases (gases with a surface mixing ratio on the order of parts per million by volume (ppmv = 10^{-6}) or less) is more recent (Lovelock and Margulis, 1974; Margulis and Lovelock, 1974; Margulis and Lovelock, 1978). Important trace atmospheric gases of biogenic origin include methane (CH_4), ammonia (NH_3), hydrogen sulfide (H_2S), and nitrous oxide (N_2O).

For many years it has been assumed that the Earth's prebiological paleoatmosphere was strongly reducing, containing large amounts of methane, ammonia, hydrogen sulfide, and carbon monoxide (CO) (Hart, 1979). Over the last few years, however, geochemical and geological evidence (Walker, 1977) and photochemical/chemical considerations (Levine, 1982) have favored a more mildly reducing mixture of molecular nitrogen, carbon dioxide, and water vapor (H_2O) for the composition of the prebiological paleoatmosphere. Methane, ammonia, hydrogen sulfide, and carbon monoxide are all important trace gases in the present atmosphere and impact atmospheric photochemistry and chemistry. With the exception of carbon monoxide, these gases are overwhelmingly produced by biogenic activity in the present atmosphere. Nitrous oxide, another biogenic gas, which controls the levels of ozone (O_3) in the stratosphere will also be considered. Recent measurements indicate that atmospheric levels of methane and nitrous oxide may be increasing. Methane, nitrous oxide, and ammonia absorb Earth-emitted infrared radiation and, hence, impact the climate as well as the photochemistry/chemistry of the atmosphere. The distribution of these gases in the early atmosphere will be investigated using a photochemical model of the early atmosphere, which is described in the next section.

Thermodynamic equilibrium calculations** indicate that the levels of CH_4, NH_3,

* NASA-National Research Council Research Fellow

** Thermodynamic equilibrium concentrations are those calculated by assuming the production of a given species in thermodynamic equilibrium with a mixture of air ($N_2 = 0.78$ atm, $O_2 = 0.21$ atm, $H_2O = 0.01$ atm, and $CO_2 = 3.3 \times 10^{-4}$ atm) at atmospheric temperature (about 300 K).

Origins of Life **15** (1985) 299-318. 0046-5763/85.15.

H_2S, CO, and N_2O in the present atmosphere should be very low: CH_4 mixing ratio $= 10^{-145}$, $NH_3 = 2 \times 10^{-60}$, $H_2S = 0$, $CO = 6 \times 10^{-49}$, and $N_2O = 2 \times 10^{-19}$ (Chameides and Davis, 1982). The measured surface mixing ratios of these gases in the atmosphere ($CH_4 = 1.6 \times 10^{-6}$, $NH_3 = 1 \times 10^{-9}$, $H_2S = 4 \times 10^{-11}$, $CO = 1 \times 10^{-7}$, and $N_2O = 3 \times 10^{-7}$) is strong testimony to the important role of the biosphere as a source of trace atmospheric gases (Lovelock and Margulis, 1974).

2. Photochemical Model

To investigate the photochemistry/chemistry of CH_4, NH_3, and H_2S in the early atmosphere, we have modified our one-dimensional photochemical model of the paleoatmosphere. This model was described in a series of papers on the composition and photochemistry/chemistry of the early atmosphere (Levine *et al.*, 1982; Canuto *et al.*, 1982; and Canuto *et al.*, 1983). The photochemical/chemical processes involving CH_4, NH_3, and H_2S have been added to the chemical package that already included the detailed chemistry of the oxygen species (O_2, O_3, O, $O(^1D)$), hydrogen species (H_2, H_2O_2, HO_2, OH, and H), and carbon species (CO_2, CO, H_2CO, and HCO). Another version of the model also contains the nitrogen species (N_2O, NO, NO_2, NO_3, N_2O_5, HNO_3, HNO_2, and N), and chlorine species (HCl, CH_3Cl, CH_3CCl_3, Cl_2, CClO, ClO_2, and $ClNO_3$) (Levine *et al.*, 1981).

The following species were added in the present version of the model: CH_4, CH_3, CH_3OOH, CH_3O_2, CH_3O, NH_3, NH_2, H_2S, HS, SO_2, and HCN. The model now calculates the vertical distribution of 24 atmospheric species based on 15 photochemical processes, 68 chemical processes, and the rainout of water-soluble species. The photochemical, chemical, and rainout processes and their reaction rates are given in Table I.

For our photochemical calculations, we have assumed a background atmospheric composition resulting from the outgassing of volatiles originally trapped in the Earth's interior. These outgassed species include molecular nitrogen (N_2), water vapor (H_2O), carbon dioxide (CO_2), molecular hydrogen (H_2), carbon monoxide (CO), and sulfur dioxide (SO_2). N_2 at a partial pressure of 0.8 bar is the major atmospheric constituent. N_2 is a chemically inert species that participates in chemical reactions only as a third body (M). The H_2O vapor mixing ratio is specified in the troposphere (surface to 14.5 km) and varies from 1.2×10^{-2} at the surface to 4.6×10^{-7} at 14.5 km (the tropopause). Above the tropopause, the distribution of H_2O vapor is calculated as a chemically active species using a coupled continuity/transport equation, as are 22 other species (since $O(^1D)$ and NH_2 are chemically very shortlived, their profiles are calculated by assuming photochemical equilibrium, i.e., the vertical eddy transport term of the continuity/transport equation was neglected). For the majority of the calculations in this paper, the following lower boundary conditions on the outgassed species are used: the surface mixing ratio of CO_2 is 280 parts per million by volume (ppmv $= 10^{-6}$) (the preindustrial level of CO_2); the surface mixing ratio of H_2 is

TABLE I
Photochemical and chemical reactions in model

Reaction number	Reaction	Rate constant*
J1:	$O_2 + h\nu \rightarrow O + O$	3.0×10^{-7}
J2:	$O_3 + h\nu \rightarrow O + O_2$	2.5×10^{-4}
J3:	$O_3 + h\nu \rightarrow O(^1D) + O_2$	2.5×10^{-3}
J4:	$H_2O + h\nu \rightarrow OH + H$	1.1×10^{-6}
J5:	$H_2O_2 + h\nu \rightarrow OH + OH$	3.8×10^{-5}
J6:	$H_2CO + h\nu \rightarrow H + HCO$	4.5×10^{-5}
J7:	$H_2CO + h\nu \rightarrow H_2 + CO$	4.8×10^{-5}
J8:	$CO_2 + h\nu \rightarrow CO + O$	1.1×10^{-8}
J9:	$HCO + h\nu \rightarrow H + CO$	1.3×10^{-2}
J10:	$CH_4 + h\nu \rightarrow CH_3 + H$	4.8×10^{-8}
J11:	$NH_3 + h\nu \rightarrow NH_2 + H$	1.0×10^{-4}
J12:	$H_2S + h\nu \rightarrow HS + H$	1.5×10^{-4}
J13:	$SO_2 + h\nu \rightarrow SO + S$	5.4×10^{-4}
J14:	$CH_3OOH + h\nu \rightarrow CH_3O + OH$	3.8×10^{-5}
J15:	$HCN + h\nu \rightarrow CN + H$	1.7×10^{-6}
1	$O + O_2 + M \rightarrow O_3 + M$	$1.1 \times 10^{-34} \exp(510/T)$
2	$O + O_3 \rightarrow 2O_2$	$1.5 \times 10^{-11} \exp(-2218/T)$
3	$O(^1D) + O_2 \rightarrow O + O_2$	$3.2 \times 10^{-11} \exp(67/T)$
4	$O(^1D) + N_2 \rightarrow O + N_2$	$2.0 \times 10^{-11} \exp(107/T)$
5	$H_2O + O(^1D) \rightarrow 2OH$	2.2×10^{-10}
6	$H + O_2 + M \rightarrow HO_2 + M$	$2.1 \times 10^{-32} \exp(290/T)$
7	$H + O_3 \rightarrow OH + O_2$	$1.4 \times 10^{-10} \exp(-470/T)$
8	$OH + O \rightarrow H + O_2$	$2.2 \times 10^{-11} \exp(117/T)$
9	$OH + O_3 \rightarrow HO_2 + O_2$	$1.6 \times 10^{-12} \exp(-940/T)$
10	$OH + OH \rightarrow H_2O + O$	$4.2 \times 10^{-12} \exp(-242/T)$
11	$HO_2 + O \rightarrow OH + O_2$	$3.0 \times 10^{-11} \exp(200/T)$
12	$HO_2 + O_3 \rightarrow OH + 2O_2$	$1.4 \times 10^{-14} \exp(-580/T)$
13	$HO_2 + OH \rightarrow H_2O + O_2$	4.0×10^{-11}
14	$HO_2 + HO_2 \rightarrow H_2O_2 + O_2$	2.5×10^{-12}
15	$H_2O_2 + OH \rightarrow HO_2 + H_2O$	$3.1 \times 10^{-12} \exp(-187/T)$
16	$O(^1D) + H_2 \rightarrow OH + H$	1.0×10^{-10}
17	$OH + OH + M \rightarrow H_2O_2 + M$	See JPL Publication 82-57 (1982)
18	$H_2O_2 + O \rightarrow OH + HO_2$	$1.0 \times 10^{-11} \exp(-2500/T)$
19	$H_2 + OH \rightarrow H_2O + H$	$6.1 \times 10^{-12} \exp(-2030/T)$
20	$H_2CO + OH \rightarrow HCO + H_2O$	1.0×10^{-11}
21	$H_2CO + O \rightarrow OH + HCO$	$3.0 \times 10^{-11} \exp(-1550/T)$
22	$HCO + O_2 \rightarrow CO + HO_2$	$3.5 \times 10^{-12} \exp(140/T)$
23	$CO + OH \rightarrow H + CO_2$	See JPL Publication 82-57 (1982)
24	$O + O + M \rightarrow O_2 + M$	$2.8 \times 10^{-34} \exp(710/T)$
25	$H + H + M \rightarrow H_2 + M$	8.3×10^{-33}
26	$H_2 + O \rightarrow OH + H$	$3.0 \times 10^{-14} \exp(-4480/T)$
27	$H + HO_2 \rightarrow O_2 + H_2$	1.4×10^{-11}
28	$H + HO_2 \rightarrow H_2O + O$	9.4×10^{-13}
29	$H + HO_2 \rightarrow OH + OH$	3.2×10^{-11}
30	$H + CO + M \rightarrow HCO + M$	$2.0 \times 10^{-33} \exp(-850/T)$
31	$H + HCO \rightarrow H_2 + CO$	3.0×10^{-10}
32	$HCO + HCO \rightarrow H_2CO + CO$	6.3×10^{-11}
33	$OH + HCO \rightarrow H_2O + CO$	5.0×10^{-11}
34	$O + HCO \rightarrow H + CO_2$	1.0×10^{-10}
35	$O + HCO \rightarrow OH + CO$	1.0×10^{-10}
36	$HO_2 + HCO \rightarrow H_2O_2 + CO$	1.0×10^{-11}

Table I - Continued

Reaction number	Reaction	Rate constant*
37	$H_2CO + H \rightarrow H_2 + HCO$	$2.8 \times 10^{-11} \exp(-1540/T)$
38	$CH_4 + OH \rightarrow CH_3 + H_2O$	$2.4 \times 10^{-12} \exp(-1710/T)$
39	$CH_4 + O(^1D) \rightarrow CH_3 + OH$	1.4×10^{-10}
40	$CH_4 + O(^1D) \rightarrow H_2CO + H_2$	1.4×10^{-10}
41	$CH_3 + H + M \rightarrow CH_4 + M$	$3.3 \times 10^{-10}/[1 + 1/(2 \times 10^{-19}[M])]$
42	$CH_3 + O_2 + M \rightarrow CH_3O_2 + M$	$2.6 \times 10^{-31}[M]$
43	$CH_3O_2 + HO_2 \rightarrow CH_3OOH + O_2$	$7.7 \times 10^{-14} \exp(1300/T)$
44	$CH_3OOH + OH \rightarrow CH_3O_2 + H_2O$	$2.6 \times 10^{-12} \exp(-190/T)$
45	$CH_3O + O_2 \rightarrow H_2CO + HO_2$	$1.2 \times 10^{-13} \exp(-1350/T)$
46	$CH_3 + OH \rightarrow H_2CO + H_2$	1.0×10^{-10}
47	$CH_3 + O \rightarrow H_2CO + H$	1.4×10^{-10}
48	$CH_3 + CH_3 + M \rightarrow C_2H_6 + M$	5.5×10^{-11}
49	$NH_3 + OH \rightarrow NH_2 + H_2O$	$2.3 \times 10^{-12} \exp(-800/T)$
50	$NH_3 + O \rightarrow NH_2 + OH$	$6.6 \times 10^{-12} \exp(-3300/T)$
51	$NH_3 + O(^1D) \rightarrow NH_2 + OH$	2.5×10^{-10}
52	$NH_3 + H \rightarrow NH_2 + H_2$	1.0×10^{-16}
53	$NH_2 + OH \rightarrow NH_3 + O$	1.0×10^{-13}
54	$NH_2 + H_2 \rightarrow NH_3 + H$	1.0×10^{-16}
55	$NH_2 + H + M \rightarrow NH_3 + M$	$6.0 \times 10^{-30}[M]/\{1 + 3 \times 10^{-20}[M]\}$
56	$NH_2 + NH_2 + M \rightarrow N_2H_4 + M$	1.0×10^{-10}
57	$NH_2 + O \rightarrow HNO + H$	1.8×10^{-12}
58	$NH_2 + O \rightarrow NO + OH$	1.8×10^{-12}
59	$H_2S + OH \rightarrow HS + H_2O$	$5.9 \times 10^{-12} \exp(-65/T)$
60	$H_2S + O \rightarrow HS + OH$	$1.0 \times 10^{-11} \exp(-1810/T)$
61	$H_2S + H \rightarrow HS + H_2$	$1.3 \times 10^{-11} \exp(860/T)$
62	$HS + O \rightarrow H + SO$	1.6×10^{-10}
63	$HS + O_2 \rightarrow OH + SO$	3.2×10^{-15}
64	$HS + H \rightarrow H_2 + S$	2.5×10^{-11}
65	$HS + HS \rightarrow H_2S + S$	1.2×10^{-11}
66	$SO_2 + OH + M \rightarrow HSO_3 + M$	$3.0 \times 10^{-31}(T/300)^{-2.9}[M]$
67	$HCN + OH \rightarrow H_2O + CN$	2.0×10^{-15}
68	$HCN + O \rightarrow OH + CN$	1.1×10^{-17}
69	H_2CO, H_2O_2, CH_3OOH, NH_3 rainout	$1.0 \times 10^{-6}\,s^{-1}$

* Photolysis rates (J1–J15) are for the top of the atmosphere (53.5 km in the model) in units of s^{-1}. Two body kinetic reactions are in units of $cm^3\ molec^{-1}s^{-1}$; three body kinetic reactions are in units of $cm^6\ molec^{-1}s^{-1}$. M represents any third body (usually N_2). Kinetic reaction rates and photochemical parameters were taken from: *Chemical Kinetics and Photochemical Data for Use in Stratospheric Modeling* by Demore, W. B., Watson, R. T., Golden, D. M., Hampson, R. F., Kurylo, M., Howard, C. J., Molina, M. J., and Ravishankara, A. R., JPL publication 82-57, July 15, 1982 (186 pages) and Evaluated Kinetic and Photochemical Data for Atmospheric Chemistry: Supplement 1 by Baulch, D. L., Cox, R. A., Crutzen, P. J., Hampson, R. F., Kerr, J. A., Troe, J., and Watson, R. T., *Journal of Physical and Chemical Reference* **11**, No. 2, 1982, pp. 327-496.

17 ppmv (Kasting and Walker, 1981); the surface volcanic flux of CO is 2×10^8 molec. $cm^{-2} s^{-1}$ (Kasting and Walker, 1981); and the surface volcanic flux of SO_2 varies from 1×10^9 to 1×10^{12} molec. $cm^{-2} s^{-1}$. Superimposed on this atmospheric mixture are surface fluxes of CH_4, NH_3, and H_2S. Calculations were performed for different surface fluxes of CH_4, NH_3, and H_2S ranging from 1×10^9 to 1×10^{12} molec. $cm^{-2} s^{-1}$.

The U.S. Standard Atmosphere Mid-Latitude Spring/Autumn temperature profile is specified in the troposphere. An early atmosphere temperature profile for the O_3-deficient stratosphere that decreases linearly from the tropopause to the mesopause (80 km) is used. This temperature profile is based on coupled photochemical-radiative equilibrium temperature calculations (Levine and Boughner, 1979). The vertical eddy diffusion coefficient profile of McElroy *et al.* (1974) is used. Photodissociation rates are diurnally averaged for a latitude of 30° and solar declination of 0° (Rundel, 1977). The model includes the solar spectrum from 110 to 735 nm based on the fluxes of Ackerman (1971). The one-dimensional photochemical model extends from the surface to 53.5 km with 1 km spatial resolution between the surface and 10 km, and 1.5 km spatial resolution between 10 and 53.5 km.

3. Methane (CH_4)

Thermodynamic equilibrium calculations indicate that the mixing ratio of CH_4 should be about 10^{-145} (Chameides and Davis, 1982). CH_4 with a mean global surface mixing ratio of about 1.66 ppmv (10^{-6}) is the most abundant atmospheric carbon species after carbon dioxide (mixing ratio = 330 ppmv) in the present atmosphere. The 139 order of magnitude enhancement in atmospheric CH_4 over its calculated equilibrium value indicates the importance of biogenic processes as sources of atmospheric species. CH_4 is biologically produced by the decay of organic matter by anaerobic bacteria in anoxic environments rich in organic matter, such as waterlogged soils, swamps, marshes, freshwater and marine sediments, as well as in the intestines of animals (enteric fermentation in ruminants). Estimates of the sources of atmospheric CH_4 and their global production rates (in units of 10^{14} g CH_4/yr) are rice paddy fields, 0.7–1.2; natural wetlands, 0.3–2.2; enteric fermentation in ruminants, 0.6; biomass burning, 0.3–1.1; and gas leakages, 0.5 (Baulch *et al.*, 1982). These estimates yield a total global CH_4 production rate of $2.4–5.6 \times 10^{14}$ g CH_4/yr.

Measurements indicate that CH_4 exhibits a constant mixing ratio throughout the entire troposphere. Recent measurements indicate that atmospheric CH_4 may be increasing (Graedel and McRae, 1980; Rasmussen and Khalil, 1981). On the basis of 22 months of almost continuous measurements, Rasmussen and Khalil found that CH_4 is increasing about 2.0 ± 0.5 % per year. In an analysis of all measurements made between 1965 and 1980, they found an average increase of about 1.7 % per year. Analyses of CH_4 trapped in polar ice cores as far back as 27 000 years ago indicate that atmospheric CH_4 remained fairly constant at about 0.7 ppmv from 27 000 years ago to about the year 1580 (Craig and Chou, 1982). Beginning in 1580, CH_4 levels began to increase at about 0.114 ppmv per century until about 1915, at which time CH_4 began

increasing at a faster rate of about 2.5 ppmv per century, which is roughly equivalent to an increase of about 1.7 % per year (Craig and Chou, 1982). This global increase in CH_4 is very puzzling. CH_4 is a key species in the photochemistry/chemistry of the troposphere and affects tropospheric levels of ozone, the hydroxyl radical (OH), and carbon monoxide (Logan *et al.*, 1981; Levine and Allario, 1982). In addition, CH_4 absorbs Earth-emitted infrared radiation at about 7.7 μm within the 'atmospheric window' (7–14 μm). An increase in CH_4 from 0.7 ppmv to its present value of about 1.66 ppmv may have caused an increase in the global temperature of the Earth of about 0.23 °C (Wang *et al.*, 1976), which is about half of the temperature increase calculated to have occurred as a result of increases in CO_2.

For many years, it was believed that the prebiological paleoatmosphere was strongly reducing, consisting of CH_4, ammonia (NH_3), hydrogen sulfide (H_2S), and carbon monoxide (CO). Hart (1979) suggested the following composition for the prebiological paleoatmosphere: CH_4 = 13 %; NH_3 = 27 %; H_2S = 20 %; and CO = 40 %. This prebiological paleoatmosphere of Hart had a total mass of 15×10^{21} g, compared to the mass of present atmosphere of about 5.136×10^{21} g. The amount of CH_4, NH_3, H_2S, and CO in the present atmosphere is compared with the amount hypothesized to have been present in the paleoatmosphere (Hart, 1979) in Table II. Various geochemical and geological considerations no longer support the hypothesis of a strongly reducing prebiological paleoatmosphere of CH_4, NH_3, H_2S, and CO (see, for example, Walker, 1977). Instead, a mildly reducing prebiological paleoatmosphere composed of molecular nitrogen (N_2), carbon dioxide (CO_2), and water vapor (H_2O), the major constituents of volcanic emissions, is suggested based on geochemical and geological considerations (Walker, 1977). But what about the presence of smaller amounts of CH_4, NH_3, H_2S, and CO in the prebiological paleoatmosphere?, and secondly, what were the possible sources of CH_4, NH_3, H_2S, and CO in the prebiological paleoatmosphere? These gases may have resulted (1) as a remnant from the primordial solar nebula, (2) via outgassing from the Earth's interior, (3) via atmospheric photo-

TABLE II
Gases in the prebiological and present atmosphere

	Prebiological paleoatmosphere (grams) (Hart, 1979)	Present atmosphere		
		Calculated mixing ratio[1]	Measured mixing ratio[2]	Amount[2] (grams)
Methane (CH_4)	2×10^{21}	10^{-145}	$\sim 1.5 \times 10^{-6}$	$\sim 4.3 \times 10^{15}$
Ammonia (NH_3)	4×10^{21}	2×10^{-60}	$\sim 1 \times 10^{-8}$	$\sim 3 \times 10^{13}$
Hydrogen sulfide (H_2S)	3×10^{21}	–	$\sim 2 \times 10^{-10}$	$\sim 1.2 \times 10^{12}$
Carbon monoxide (CO)	6×10^{21}	6×10^{-49}	$\sim 1.2 \times 10^{-7}$	$\sim 5.9 \times 10^{14}$
Nitrous oxide (N_2O)	–	2×10^{-19}	$\sim 3 \times 10^{-7}$	$\sim 2.3 \times 10^{15}$
Total mass of atmosphere	15×10^{21}			5.136×10^{21}

[1] Based on thermodynamic equilibrium calculations (Chameides and Davis, 1982)
[2] Walker (1977)

chemical/chemical processes, (4) via cometary influx, and (5) from surface catalytic reactions. We can readily eliminate several of these sources. There is geochemical evidence to indicate that the early atmosphere was not a remnant of the primordial solar nebula, but resulted from the outgassing of volatiles trapped in the interior. Furthermore, it does not appear that significant levels of CH_4, NH_3, H_2S, and CO ever outgassed from the interior. In addition, with the exception of CO which results from the photolysis of CO_2, these gases are not produced via atmospheric photochemical/chemical processes. While comets have been suggested a source of volatiles to the early atmosphere (Oró, 1961), their contribution has not been accurately assessed. Surface catalytic reactions involving the fixation of atmospheric nitrogen by naturally occurring titanium oxide in sand may have been a localized source of NH_3 (Henderson-Sellers and Schwartz, 1980), although it does not appear to be an important source on a global scale. To investigate the photochemistry, distribution, and stability of these gases in the prebiological paleoatmosphere, we have arbitrarily specified a surface source of unknown origin for our photochemical calculations.

The photochemistry/chemistry, stability, and lifetime of CH_4 in the prebiological paleoatmosphere were investigated and reported at the Sixth College Park Colloquium on Chemical Evolution in October 1981 (Levine *et al.*, 1982). This study showed that in the upper atmosphere (above 100 km), the lifetime of CH_4 is controlled by its photolytic destruction by solar ultraviolet radiation (reaction (1)). The mean atmospheric lifetime of CH_4 against photolytic destruction above 100 km was found to be on the order of a few days . On the other hand, near the surface, the lifetime of CH_4 against photolytic destruction was found to be infinitely long, due primarily to the shielding of CH_4 by atmospheric H_2O. However, it was shown that the lifetime of CH_4 near the surface was controlled by its reaction with the hydroxyl radical (OH) (reaction (2)). The lifetime of CH_4 against destruction by OH was found to be about 50 years (about a factor of five greater than its lifetime in the present atmosphere). The study of Levine *et al.* (1982) concluded that in the absence of a continuous source, the presence of CH_4 in the prebiological paleoatmosphere was extremely shortlived, if it ever existed at all. In this paper, we will present theoretical photochemical calculations of the vertical distribution of CH_4 in the prebiological paleoatmosphere for different assumed surface fluxes of CH_4 of unspecified origin. CH_4 is destroyed by direct photolysis (reaction (1)) and by reactions with the hydroxyl radical (OH) and excited atomic oxygen ($O(^1D)$) (reactions (2)–(4):

$$CH_4 + h\nu \rightarrow CH_3 + H \; (\lambda \leq 145\,\text{nm}) \tag{1}$$

$$CH_4 + OH + CH_3 + H_2O \tag{2}$$

$$CH_4 + O(^1D) \rightarrow CH_3 + OH \tag{3}$$

$$CH_4 + O(^1D) \rightarrow CH_2O + H_2. \tag{4}$$

The OH needed in reaction (2) is formed from H_2O via direct photolysis and by reaction with $O(^1D)$:

$$H_2O + h\nu \rightarrow OH + H \ (\lambda \leq 240\,nm) \tag{5}$$

$$H_2O + O(^1D) \rightarrow 2OH \tag{6}$$

In the oxygen-deficient prebiological paleoatmosphere, the direct photolysis of H_2O (reaction (5)) was an important source of OH. The methyl radical (CH_3) formed in reactions (1) to (4) may reform CH_4 via reaction with atomic hydrogen (H):

$$CH_3 + H + M \rightarrow CH_4 + M. \tag{7}$$

However, there are other competing reactions, involving OH and atomic oxygen (O) that form formaldehyde (H_2CO) (reactions (8) and (9)), with CH_3 itself that forms ethane (C_2H_6) (reaction (10)), and with O_2 that forms the methylperoxyl radical (CH_3O_2) (reaction (11)):

$$CH_3 + OH \rightarrow H_2CO + H_2 \tag{8}$$

$$CH_3 + O \rightarrow H_2CO + H \tag{9}$$

$$CH_3 + CH_3 \rightarrow C_2H_6 \tag{10}$$

$$CH_3 + O_2 + M \rightarrow CH_3O_2 + M. \tag{11}$$

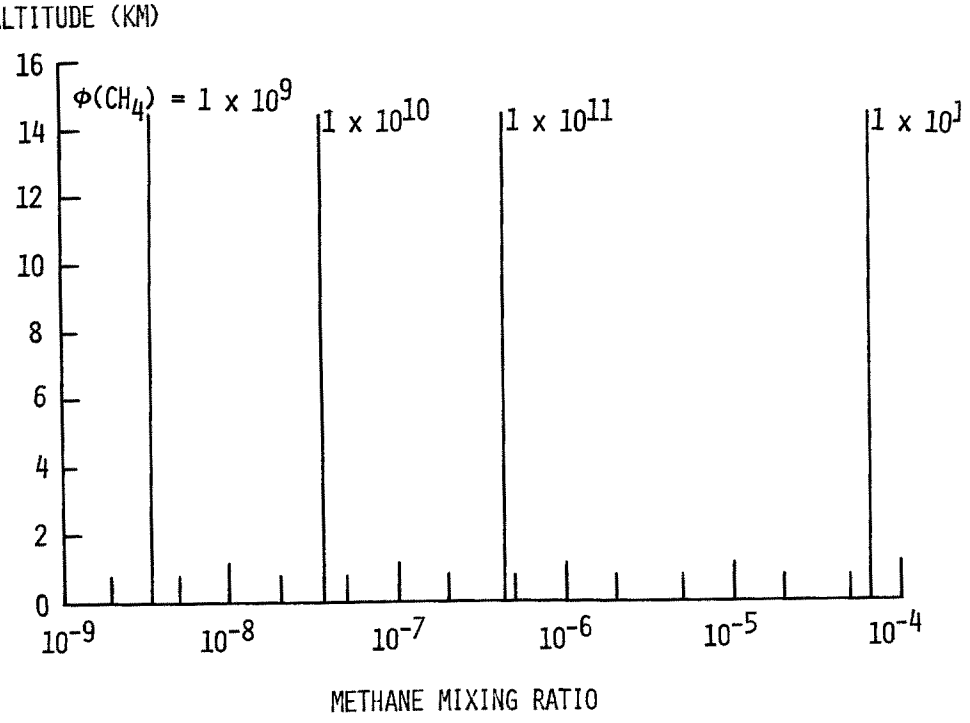

Fig. 1. Vertical distribution of CH_4 in prebiological paleoatmosphere: variation with surface CH_4 flux from 1×10^9 to 1×10^{12} molec. $cm^{-2}\,s^{-1}$.

To calculate vertical profiles of CH_4 in the prebiological troposphere, we have simultaneously solved reactions (1)–(11) for the relevant species (CH_4, CH_3, OH, O, $O(^1D)$, etc.), as well as the other species affecting their photochemistry using coupled species continuity/flux equations. For these calculations, we assumed a lower boundary surface CH_4 flux (of unspecified origin) ranging from 1×10^9 to 1×10^{12} molec. $cm^{-2}s^{-1}$. A CH_4 methane flux of 1×10^9 molec. $cm^{-2}s^{-1}$ corresponds to about 4.3×10^{12} g CH_4/yr. (For comparison, estimates of the total CH_4 flux into the present atmosphere range from 240 to 560×10^{12} g CH_4/yr (Baulch *et al.*, 1982).) Calculated CH_4 profiles are shown in Figure 1. CH_4 exhibits a constant mixing ratio with altitude throughout the troposphere since its mean atmospheric lifetime ($\sim$ 50 years) against destruction by OH is significantly greater than its vertical mixing time. Due to vigorous vertical mixing within the troposphere (resulting from its negative temperature gradient), the vertical mixing time of a species within the troposphere is about 70 days. Therefore, species with photochemical/chemical lifetimes longer than about a month, such as CH_4, will exhibit mixing ratios that do not vary with altitude within the troposphere (H_2O vapor is an exception, since its mixing ratio in the troposphere is controlled by condensation). Within a hemisphere, horizontal mixing times in the troposphere are comparable to vertical mixing times. Mixing between hemispheres takes about a year. Therefore, a species such as CH_4 with a photochemical/chemical lifetime of about 50 years will exhibit a constant mixing ratio throughout the entire global troposphere.

4. Ammonia (NH_3)

Thermodynamic equilibrium calculations indicate that the mixing ratio of NH_3 should be about 2×10^{-60} (Chameides and Davis, 1982). NH_3 with a mean global surface mixing ratio in the range of 0.1 to 1 ppbv (10^{-9}), depending on geographical region and season, is the most abundant atmospheric nitrogen species after molecular nitrogen (N_2) (78.08 % by volume) and nitrous oxide (N_2O) (330 ppbv) in the present atmosphere. As in the case of CH_4, the 51 order of magnitude enhancement in atmospheric NH_3 over its calculated equilibrium value, once again points up the importance of biogenic processes as source of atmospheric species.

Biological fixation of atmospheric nitrogen (N_2) produces organic nitrogen (RNH_2). Through mineralization, O_2 combines with RNH_2 to form ammonium (NH_4^+) in the soil. The NH_4^+ can undergo volatilization forming gaseous NH_3, which may be released to the atmosphere. NH_4^+ may also be oxidized to form nitrite (NO_2^-) by Nitrosomonas bacteria in the process of primary nitrification. NO_2^- may be further oxidized (by Nitrobacter bacteria) to form nitrate (NO_3^-) during secondary nitrification. Gaseous nitrous oxide (N_2O) and nitric oxide (NO) are direct or indirect intermediate products of these pathways. Denitrification is an anaerobic process in which NO_3^- is reduced to NO_2^-, and eventually to NH_4^+, or gaseous N_2, with N_2O and NO as intermediate products. During these microbiological transformations, gaseous NH_3, N_2, N_2O, and NO are formed and released to the atmosphere.

Dawson (1977) has estimated the total production of NH_3 due to the volatilization of NH_4^+ from non-fertilized fields to be about 50×10^{12} g NH_3/yr. Baulch *et al.* (1982) give a somewhat lower estimate of $< 30 \times 10^{12}$ g N/yr. Estimates for other sources of NH_3 (in units of 10^{12} g N/yr) include domestic animals, 10–20; wild animals, 2–6; fertilized fields, < 3; burning 4–12; and biomass burning, < 60 (Baulch *et al.*, 1982). These estimates yield a total NH_3 production rate of about 100×10^{12} g N/yr.

Measurements indicate that atmospheric NH_3 is very variable with geographical region, season, and soil and meteorological conditions (Hoell *et al.*, 1980, 1982; Levine *et al.*, 1980). The atmospheric lifetime of NH_3, a very water soluble species, appears to be controlled by rainout with a characteristic lifetime of about 10 days (Levine *et al.*, 1980). Because the characteristic residence time of NH_3 (10 days) is short compared to its characteristic vertical and horizontal mixing times (70 days), we would expect a non-homogeneous concentration of NH_3 within the troposphere. The limited measurement set of NH_3 suggests that this is so (Hoell *et al.*, 1980, 1982).

NH_3 is the only gaseous basic constituent of the troposphere, a usually acidic environment due to the presence of the following acids: carbonic (H_2CO_3), sulfuric (H_2SO_4), nitric (HNO_3), and nitrous (HNO_2). By virtue of its high solubility, NH_3 neutralizes the ever-present tropospheric acids and, hence, neutralizes the pH of cloud droplets and the acidity of rain and snow. By reaction with nitric and sulfuric acids, NH_3 forms ammonium nitrate (NH_4NO_3) and ammonium sulfate ($(NH_4)_2SO_4$) aerosols. The loss of NH_3 via rainout, aerosol formation, and dry deposition is an additional but minor source of ammonium (NH_4^+) to the biosphere (compared to the mineralization of RNH_2). In addition to its role in the atmospheric chemistry, NH_3 absorbs Earth-emitted infrared radiation within the 'atmospheric window' and, hence, affects the climate of the Earth (Wang *et al.*, 1976).

The photochemistry/chemistry of NH_3 in the prebiological paleoatmosphere will be considered. NH_3 is destroyed by direct photolysis (reaction (12)) and by reactions with OH, H, O, and $O(^1D)$ (reactions (13)–(16)):

$$NH_3 + h\nu \leftarrow NH_2 + H \ (\lambda \leq 230\,\text{nm}) \tag{12}$$

$$NH_3 + OH \rightarrow NH_2 + H_2O \tag{13}$$

$$NH_3 + H \rightarrow NH_2 + H_2 \tag{14}$$

$$NH_3 + O \rightarrow NH_2 + OH \tag{15}$$

$$NH_3 + O(^1D) \rightarrow NH_2 + OH. \tag{16}$$

The amine radical (NH_2) formed in the above reactions may reform NH_3 via reactions with H, H_2, and OH (reactions (17)–(19)):

$$NH_2 + H + M \rightarrow NH_3 + M \tag{17}$$

$$NH_2 + H_2 \rightarrow NH_3 + H \tag{18}$$

$$NH_2 + OH \rightarrow NH_3 + O. \tag{19}$$

However, there are other competing reactions including the reaction of NH_2 with itself to form hydrazine (N_2H_4) and with O (reactions (20)–(22)):

$$NH_2 + NH_2 + M \rightarrow N_2H_4 + M \tag{20}$$

$$NH_2 + O \rightarrow HNO + H \tag{21}$$

$$NH_2 + O \rightarrow NO + OH. \tag{22}$$

To calculate vertical profiles of NH_3 in the prebiological paleoatmosphere, we have simultaneously solved reactions (12)–(22) for the relevant species. For these calculations we assumed a lower boundary surface NH_3 flux (of unspecified origin) ranging from 1×10^9 to 1×10^{12} molec. $cm^{-2} s^{-1}$. An NH_3 flux of 1×10^9 molec. $cm^{-2} s^{-1}$ corresponds to about 3.75×10^{12} g N/yr (for comparison, estimates of the total NH_3 flux into the present atmosphere are about 100×10^{12} g N/yr (Baulch *et al.*, 1982)). These calculations are shown in Figure 2. The vertical profiles of NH_3 shown in this figure are very similar to those of Kuhn and Atreya (1979) and Kasting (1982). The calculations of Kuhn and Atreya (1979) and Kasting (1982) were performed for a specified surface mixing ratio of NH_3 at the lower boundary, whereas the present calculations were performed for a specified surface flux. The present calculations also include the presence of CH_4, H_2S, and SO_2 in the prebiological paleoatmosphere, gases which were omitted in the two earlier studies of NH_3. Our calculations indicate that the mixing ratio of NH_3 is constant throughout the troposphere for mixing ratios $\geq 10^{-5}$, and that the NH_3 mixing ratio begins to decrease with altitude for surface mixing ratios of $< 10^{-5}$. In general, rainout is the major atmospheric loss mechanism for NH_3, with a mean atmospheric residence time against rainout of about 10 days (Levine *et al.*, 1980). The NH_3 residence time against photolytic destruction varies

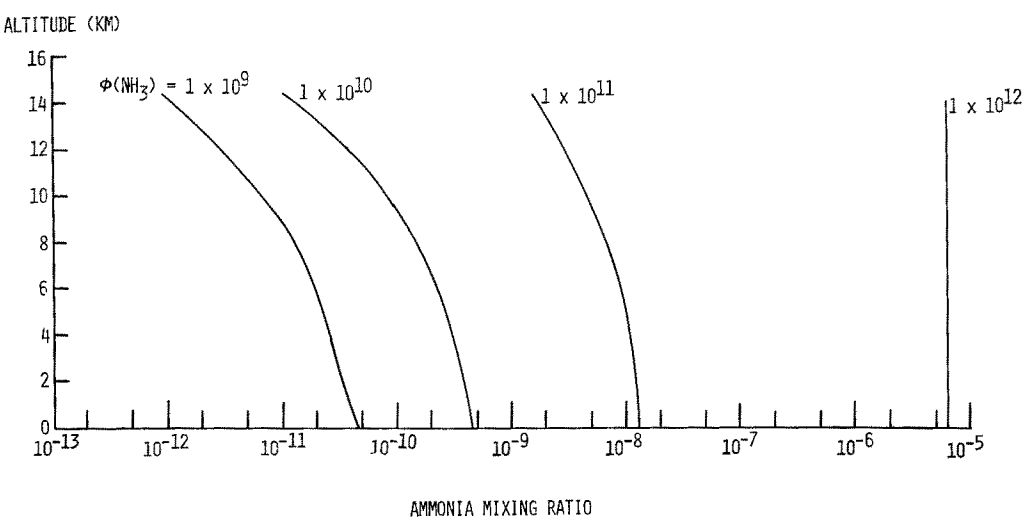

Fig. 2. Vertical distribution of NH_3 in prebiological paleoatmosphere: variation with surface NH_3 flux from 1×10^9 to 1×10^{12} molec. $cm^{-2} s^{-1}$.

from about 2.5×10^4 s (0.3 day) for a surface mixing ratio of 10^{-8} to about 6.7×10^7 s (2.1 yr) for a surface mixing of 10^{-5}. The situation is not unlike that in the present troposphere. In the present oxygen/ozone atmosphere, radiation shorter than 300 nm cannot penetrate into the troposphere, and, hence, the photolysis of NH_3 which begins shortward of 230 nm is not operable. Instead, the atmospheric loss of NH_3 is totally dominated by rainout (Levine *et al.*, 1980). After the loss due to rainout, the reaction with OH (reaction (13)) is the most important loss mechanism for NH_3 in the present atmosphere, with a mean characteristic loss time of about 40 days (Levine *et al.*, 1980).

5. Hydrogen Sulfide (H_2S)

Compared to our understanding of the biogeochemical/atmospheric cycling of the carbon, nitrogen, and oxygen species, there are fundamental deficiences in our knowledge of the sulfur cycle. These deficiencies include precise information on the atmospheric concentrations of these species, the photochemical/chemical processes that control their atmospheric distributions, and their sources and source strengths. The major sulfur species and their approximate surface mixing ratios in the present atmosphere are carbonyl sulfide (COS = 600 pptv) (pptv = 10^{-12}), sulfur dioxide (SO_2 = 100 pptv), hydrogen sulfide (H_2S = 100 pptv), and carbon disulfide (CS_2 = 40 pptv) (McElroy *et al.*, 1980; Baulch *et al.*, 1982). For comparison, thermodynamic equilibrium calculations indicate that these gases should not be present at all in the atmosphere (Chameides and Davis, 1982).

H_2S is produced by bacteria in anaerobic, sulfate-rich environments, such as marine sediments and coastal mud flats. Although the biogenic source strength of H_2S is uncertain, a value on the order of 14×10^{12} g H_2S/yr has been suggested (McElroy *et al.*, 1980). Present atmospheric levels of H_2S are controlled by its rapid reaction with OH, resulting in an atmospheric lifetime of H_2S of about 1 day (McElroy *et al.*, 1980). Photochemical calculations and the few measurements available indicate that the mixing ratio of H_2S decreases very rapidly in the lower troposphere.

The photochemistry/chemistry of H_2S in the prebiological paleoatmosphere will be considered. H_2S is destroyed by direct photolysis (reaction (23)) and by reactions with OH, O, and H (reactions (24)–(26)):

$$H_2S + h\nu \rightarrow HS + H \ (\lambda \leq 272\,\text{nm}) \tag{23}$$

$$H_2S + OH \rightarrow HS + H_2O \tag{24}$$

$$H_2S + O \rightarrow HS + OH \tag{25}$$

$$H_2S + H \rightarrow HS + H_2. \tag{26}$$

The thiohydroxyl radical (HS) formed in the above reactions may reform H_2S via reaction with itself:

$$HS + HS \rightarrow H_2S + S. \tag{27}$$

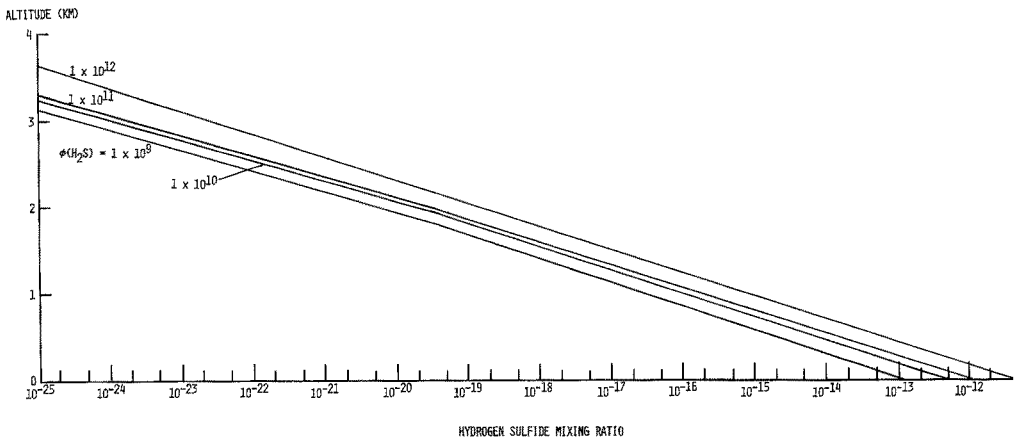

Fig. 3. Vertical distribution of H_2S in prebiological paleoatmosphere: variation with surface H_2S flux from 1×10^9 to 1×10^{12} molec. $cm^{-2}\,s^{-1}$.

However, there are additional competing reactions involving O, O_2, and H:

$$HS + O \rightarrow H + SO \tag{28}$$

$$HS + O_2 \rightarrow OH + SO \tag{29}$$

$$HS + H \rightarrow H_2 + S. \tag{30}$$

To calculate the vertical profile of H_2S in the prebiological troposphere, we have simultaneously solved reactions (23)–(30) for the relevant species. For these calculations, we assumed a lower boundary H_2S flux (of unspecified origin) ranging from 1×10^9 to 1×10^{12} molec. $cm^{-2}\,s^{-1}$. An H_2S flux of 1×10^9 molec. $cm^{-2}\,s^{-1}$ corresponds to about 9.3×10^{12} g H_2S/yr (for comparison, the flux of H_2S into the present atmosphere has been estimated to be about 14×10^{12} g H_2S/yr (McElroy *et al.*, 1980)). These calculations are shown in Figure 3. Inspection of this figure indicates that the mixing ratio of H_2S decreases very rapidly with altitude, decreasing by about 13 orders of magnitude from the surface to about 3 km. The lifetime of H_2S in the prebiological paleoatmosphere was controlled by its photolytic destruction (reaction (23)), with a characteristic residence time of less than a day.

6. Carbon Monoxide (CO)

Thermodynamic equilibrium calculations indicate that the mixing ratio of CO should be about 6×10^{-49} (Chameides and Davis, 1982). The actual measured concentration of CO in the present troposphere exhibits a marked hemispheric asymmetry with a surface mixing ratio of about 80 ppbv in the Southern Hemisphere, about 150 ppbv between the Equator and 30° N, and about 200 ppbv between 30° and 60° N (Logan *et al.*, 1981).

Sources of CO to the global atmosphere (in units of 10^{14} g CO/yr) include biomass

burning, 4–16; industrial activities, 6.4; the oxidation of CH_4, 6; and the oxidation of isoprene (C_5H_8) and terpenes ($C_{10}H_{16}$), 4–13 (Baulch *et al.*, 1982). The measured asymmetry of CO in the global troposphere is a result of the latitudinal distribution of its sources, particularly its anthropogenic sources (industrial activities), coupled with its short atmospheric lifetime of about 65 days.

The photochemistry/chemistry of CO in the prebiological paleoatmosphere will be considered. The photolysis of CO_2 (reaction (31)) leads to the production of CO:

$$CO_2 + h\nu \rightarrow CO + O \ (\lambda \leq 230\,\text{nm}) \tag{31}$$

CO is lost via chemical reactions with OH (the overwhelming sink) and with H, which leads to the formation of HCO and eventually to formaldehyde (H_2CO) (and the reformation of CO) (the photochemical production of H_2CO in the prebiological paleoatmosphere is discussed in detail in Canuto *et al.*, 1983):

$$CO + OH \rightarrow CO_2 + H \tag{32}$$

$$CO + H + M \rightarrow HCO + M \tag{33}$$

$$HCO + HCO \rightarrow H_2CO + CO \tag{34}$$

We have calculated the vertical distribution of CO for two levels of CO_2: the pre-industrial level of 280 ppmv ($CO_2 = 1$) and for 100 times this value ($CO_2 = 100$). In these calculations, we have assumed a surface CO flux of 2×10^8 molec. $cm^{-2} s^{-1}$, which represents the present volcanic flux (Kasting and Walker, 1981). The results of these calculations are given in Figure 4. The surface number density of CO ranges from about $5 \times 10^{11}\,cm^{-3}$ (mixing ratio $= 2.45 \times 10^{-8}$) for $CO_2 = 1$ to about $5 \times 10^{13}\,cm^{-3}$ (mixing ratio $= 2.45 \times 10^{-6}$) for $CO_2 = 100$.

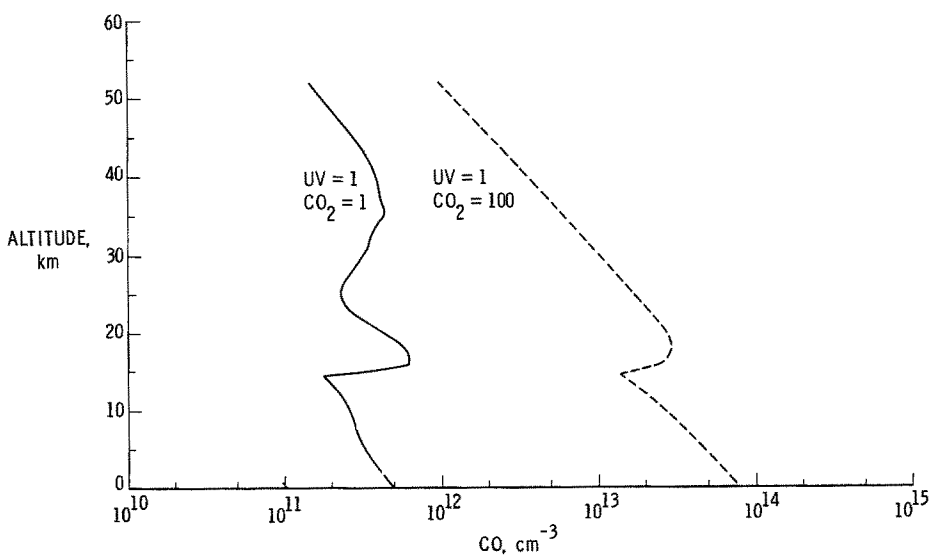

Fig. 4. Vertical distribution of CO in prebiological paleoatmosphere: variation with CO_2 level ($CO_2 = 1$ (280 ppmv) and $CO_2 = 100$ (28000 ppmv)).

The photolysis of CO_2 (reaction (31)), and the photolysis of H_2O (followed by the gravitational escape of H) led to the photochemical production of molecular oxygen (O_2) via the following reactions:

$$CO_2 + h\nu \rightarrow CO + O \ (\lambda \leq 230\,\text{nm}) \tag{31}$$

$$H_2O + h\nu \rightarrow OH + H \ (\lambda \leq 240\,\text{nm}) \tag{5}$$

$$OH + OH \rightarrow O + H_2O \tag{35}$$

$$O + O + M \rightarrow O_2 + M \tag{36}$$

$$O + OH \rightarrow O_2 + H. \tag{37}$$

The photochemical destruction of O_2 was controlled by its direct photolysis (reaction (38)) and its chemical reaction with H_2 (reaction (39)), resulting from volcanic emissions:

$$O_2 + h\nu \rightarrow O + O \ (\lambda \leq 242\,\text{nm}) \tag{38}$$

$$2H_2 + O_2 \rightarrow 2H_2O \text{ (net cycle)}. \tag{39}$$

The vertical distribution of O_2 in the prebiological paleoatmosphere was very sensitive to assumed values of CO_2, H_2, and the level of incident solar ultraviolet radiation (Canuto *et al.*, 1982, 1983). The vertical distribution of O_2 for preindustrial levels of CO_2 (280 ppmv or $CO_2 = 1$), present levels of solar ultraviolet, for two different values of H_2 mixing ratio ($H_2 = 1 \times 10^{-1}$ and 17 ppmv), is shown in Figure 5. The variation of O_2 surface mixing ratio as a function of CO_2 ($CO_2 = 1$–100) and H_2 ($H_2 = 10^{-1}$–10^{-6}) is given in Figure 6. The rates of the reactions that led to the production of O (reactions (5), (31), (35), and (38)) and their variation with altitude are shown in Figures 7 and 8. Figure 7 is for $CO_2 = 280$ ppmv ($CO_2 = 1$), $H_2 = 17$ ppmv, and present solar ultraviolet flux, and Figure 8 is for $CO_2 = 28000$ ppmv ($CO_2 = 100$),

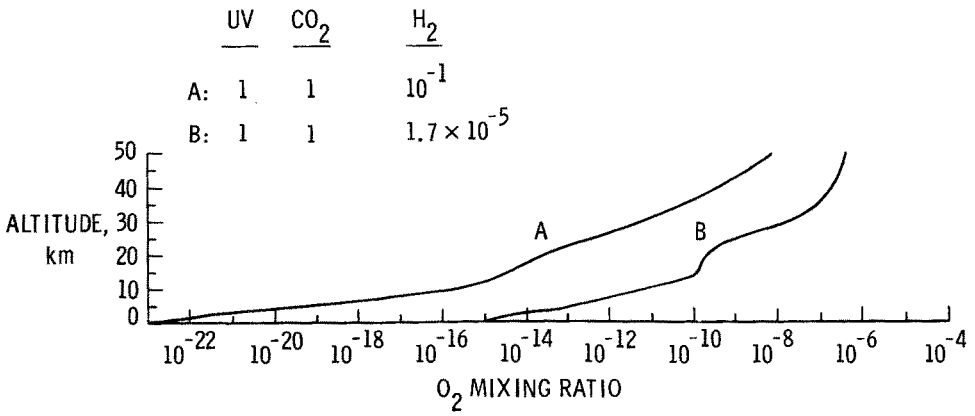

Fig. 5. Vertical distribution of O_2 in prebiological paleoatmosphere: variation with H_2 level ($H_2 = 10^{-1}$ and 17 ppmv).

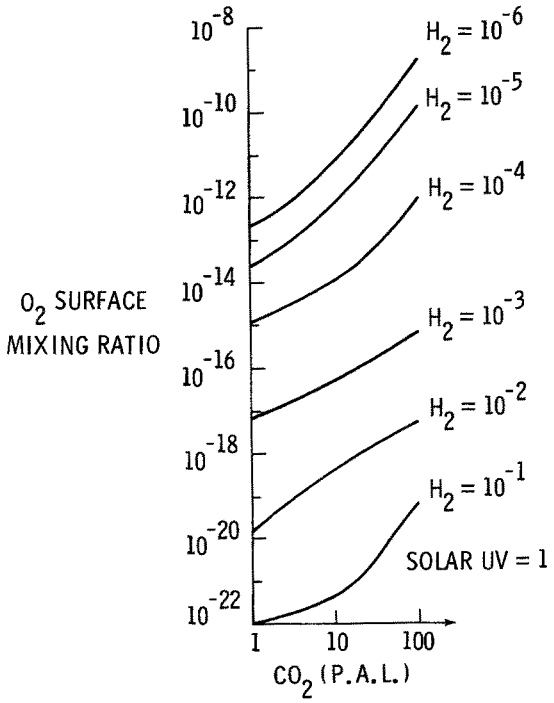

Fig. 6. Variation of O_2 surface mixing ratio as function of CO_2 (CO_2 = 1–100) and H_2 ($H_2 = 10^{-1}$–10^{-6}) in prebiological paleoatmosphere.

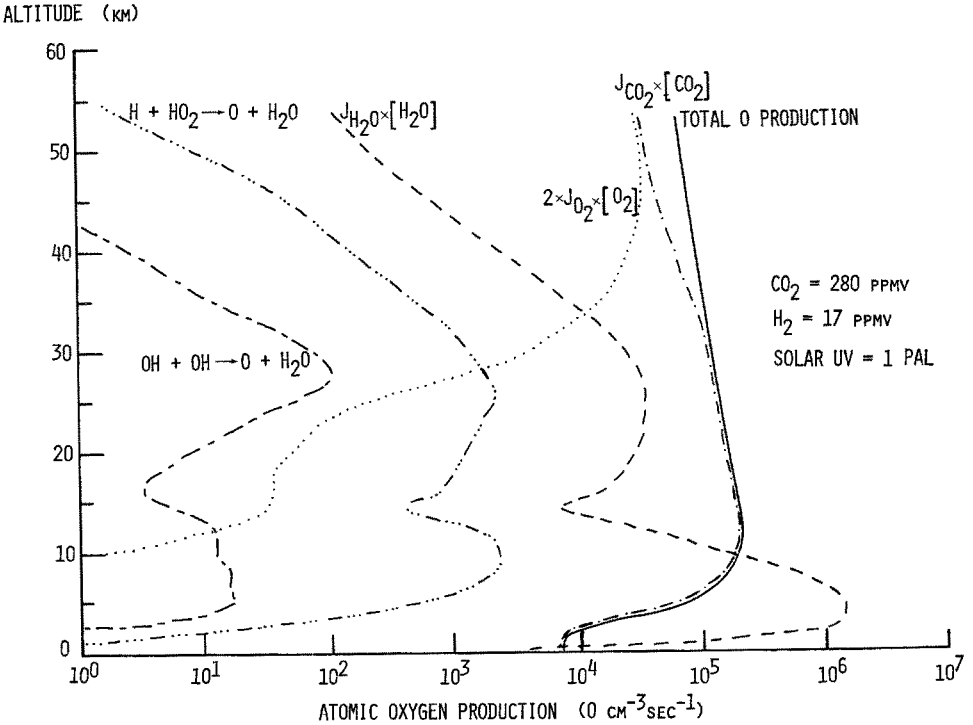

Fig. 7. Production rates of O in the prebiological paleoatmosphere for CO_2 = 1 (280 ppmv).

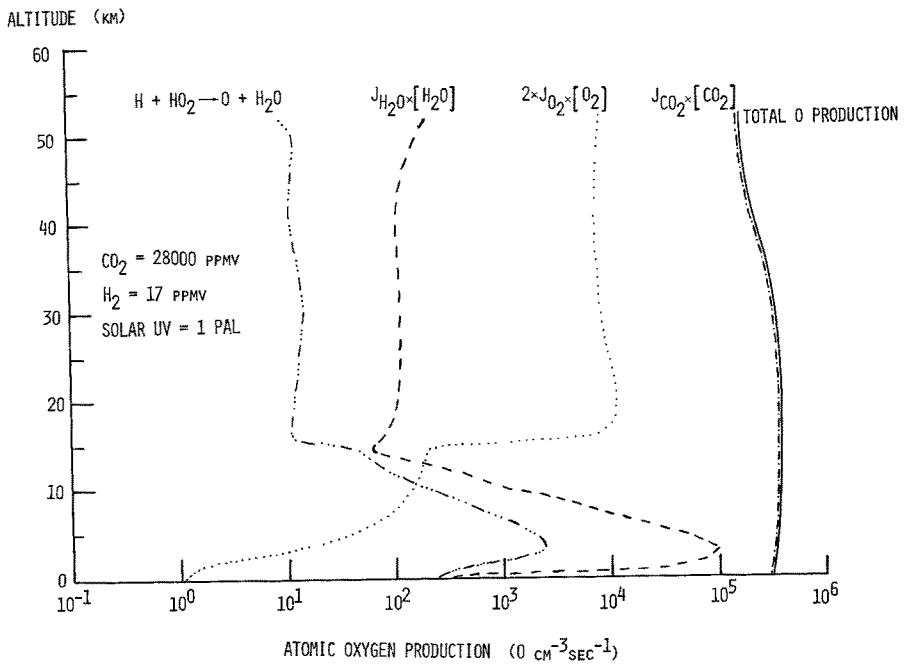

Fig. 8. Production rates of O in the prebiological paleoatmosphere for CO_2 = 100 (28000 ppmv).

H_2 = 17 ppmv, and present solar ultraviolet flux. Inspection of Figure 7 indicates that the rate of photodissociation of CO_2 (reaction (31)) is the fastest reaction involved in the photochemical production of O and O_2 above 10 km. Below 10 km, the rate of H_2O photodissociation (reaction (5)) slightly exceeds the photolysis rate of CO_2. Figure 8 indicates that the rate of photodissociation of CO_2 exceeds the rates of all of the other relevant reactions. This results from the enhanced levels of CO_2 (100 × greater than in Figure 7), which provides more CO_2 for photodissociation and at the same time, shields H_2O from photodissociation near the ground.

7. Nitrous Oxide (N_2O)

Thermodynamic equilibrium calculations indicate that the mixing ratio of N_2O should be about 2×10^{-19} (Chameides and Davis, 1982). The measured mean global surface mixing ratio of N_2O in the present atmosphere is about 3.3×10^{-7}. Measurements indicate that N_2O has been increasing between 0.2 to 0.4 %/yr (Weiss, 1981; Khalil and Rasmussen, 1983). This increase in N_2O has now been observed from measurements obtained over the last 20 years, and its origin is presumably anthropogenic – combustion of fossil fuels and agricultural fertilizer. The major source of N_2O is biogenic production via nitrification and denitrification, as discussed in the section on NH_3. The global sources of N_2O have been estimated as biogenic processes on land, 13.4×10^{12} g N/yr; biogenic processes in the oceans, 9×10^{12} g N/yr; and combustion

and agriculture, 6.6×10^{12} (for January 1978) (Khalil and Rasmussen, 1983). This results in a total global production of N_2O of about 29×10^{12} g N/yr. The combustion and agricultural (which may be about half of the combustion source) sources are increasing at a rate of about 3.5 %/yr, which may be responsible for the 0.2–0.4 %/yr increase in atmospheric N_2O (Khalil and Rasmussen, 1983). Other estimates for the global sources of N_2O include (in units of 10^{12} g N/yr): biogenic production in the oceans, 4–10; the loss of organic matter on land, 2–6; fossil fuel burning, 1.8; biomass burning, 1–2; and production in fertilized fields, < 3 (Baulch *et al.*, 1982). This results in a global production of N_2O between 10 and 20 g N/yr.

N_2O is chemically inert in the troposphere. Today, the overwhelming sink of N_2O is its photolysis in the stratosphere (however, in the oxygen/ozone deficient paleoatmosphere, photolytic destruction of N_2O was possible down to the surface):

$$N_2O + h\nu \rightarrow N_2 + O \ (\lambda \leq 337\,\text{nm}). \tag{38}$$

A small fraction of stratospheric N_2O is lost via reactions with $O(^1D)$:

$$N_2O + O(^1D) \rightarrow N_2 + O_2 \tag{39}$$

$$N_2O + O(^1D) \rightarrow 2NO. \tag{40}$$

Reaction (40) is the major source of nitric oxide (NO) in the stratosphere. NO controls the photochemical destruction of ozone (O_3) through the NO_x catalytic cycle:

$$NO + O_3 \rightarrow NO_2 + O_2 \tag{41}$$

$$NO_2 + O \rightarrow NO + O_2. \tag{42}$$

This catalytic cycle results in a net reaction of:

$$O_3 + O \rightarrow 2O_2. \tag{43}$$

In addition to its photochemical role in the destruction of stratospheric O_3, N_2O absorbs Earth-emitted infrared radiation at 7.8 μm in the 'atmospheric window' (Wang *et al.*, 1976). As a greenhouse absorber, the effect of an increase in N_2O is 10–15 % as important as the effect of an increase in CO_2 (Weiss, 1981).

The photochemistry of N_2O in the early atmosphere has been investigated by Levine *et al.* (1981). The vertical distribution of N_2O for different levels of O_2 (expressed in terms of present atmospheric level, or PAL of O_2) is shown in Figure 9 (Levine *et al.*, 1981). These calculations include reactions (38)–(40) and an assumed N_2O surface flux of $1.7 \times 10^9\,\text{cm}^{-2}\,\text{s}^{-1}$, which corresponds to a global N_2O of about 1.3×10^{13} g N/yr (for comparison, estimates for the global production of N_2O (natural and anthropogenic sources) range from about $1\text{–}3 \times 10^{13}$ g N/yr (Khalil and Rasmussen, 1983; Baulch *et al.*, 1982). These calculations indicate that in the O_2/O_3-deficient early atmosphere, the photolysis of N_2O (reaction (38)) was the overwhelming destruction mechanism for N_2O and that the production of NO via the oxidation of N_2O (reaction (40)) was a negligible source of NO. Other possible sources of NO in the early atmosphere include atmospheric lightning and biogenic production.

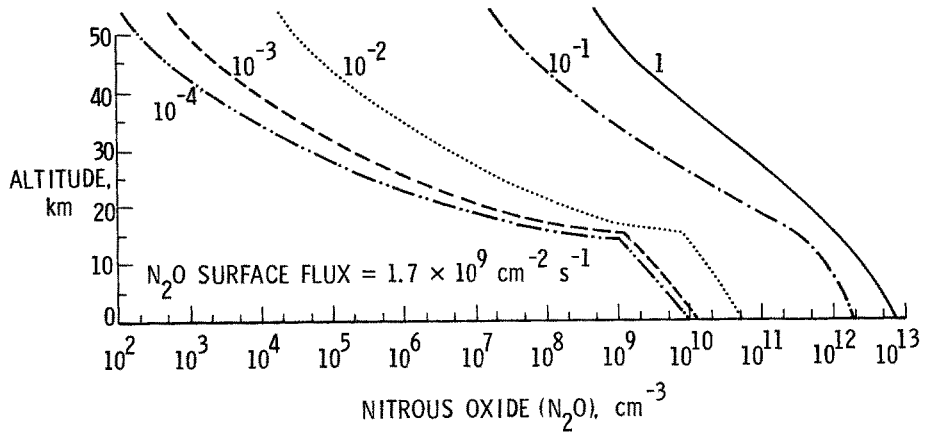

Fig. 9. Vertical distribution of N_2O in early atmosphere: variation with O_2 level (in units of present atmospheric level or PAL) (Levine *et al.*, 1981).

8. Conclusions

The photochemical calculations presented in this paper indicate that the presence of CH_4, NH_3, and H_2S (even at the parts per million level or less) in the prebiological paleoatmosphere were extremely shortlived in the absence of a continuous source. Adequate continuous sources have not been identified. There is some question whether these gases were present at all, contrary to the study of Hart (1979), who hypothesized the presence of these gases at the tens of percent level. The photochemical calculations presented here, as well as recent geological and geochemical considerations, favor a prebiological paleoatmosphere composed of N_2, CO_2, and H_2O, a composition consistent with present-day volcanic emissions. The photolysis of CO_2 would have resulted in a continuous source of atmospheric CO.

Once life evolved and diversified, the biosphere became a significant source of atmospheric gases. Even at the parts per million level or less, these gases of biogenic origin (CH_4, NH_3, H_2S, and N_2O) exert a major influence on the photochemistry of the troposphere and stratosphere. Recent measurements indicate that anthropogenic activities may be perturbing the production of these biogenic gases. Atmospheric levels of CH_4 and N_2O appear to be increasing. The increase of these gases may not only affect the photochemistry of the atmosphere, but may also impact the future climate of our planet.

Over the last decade, new ideas concerning the role and importance of the biosphere as a source of atmospheric gases have emerged. The new discipline of 'global habitability' offers the promise of treating our planet, its atmosphere, ocean, and biosphere as a single coupled system.

References

Ackermann, M.: 1971, in G. Fiocco, (ed.), *Mesospheric Models and Related Experiments*, D. Reidel, Dordrecht, Holland, pp. 149–159.

Baulch, D. L., Cox, R. A., Crutzen, P. J., Hampson, R. F., Kerr, J. A., Troe, J., and Watson, R. T.: 1982, *J. Phys. Chem. Ref. Data* **11**, 327.

Canuto, V. M., Levine, J. S., Augustsson, T. R., and Imhoff, C. L.: 1982, *Nature* **296**, 816.

Canuto, V. M., Levine, J. S., Augustsson, T. R., Imhoff, C. L., and Giampapa, M. S.: 1983, *Nature* **305**, 281.

Chameides, W. L. and Davis, D. D.: 1982, *Chem. Eng. News* **60**, 38.

Craig, H. and Chou, C. C.: 1982, *Geophys. Res. Lett.* **9**, 1221.

Dawson, G. A.: 1977, *J. Geophys. Res.* **82**, 3125.

Graedel, T. E. and McRae, J. E.: 1980, *Geophys. Res. Lett.* **7**, 977.

Hart, M. H.: 1979, *Origins of Life* **9**, 261.

Henderson- Sellers, A., and Schwartz, A. W.: 1980, *Nature* **287**, 526.

Hoell, J. M., Harward, C. N., and Williams, B. S.: 1980, *Geophys. Res. Lett.* **7**, 313.

Hoell, J. M., Levine, J. S., Augustsson, T. R., and Harward, C. N.: 1982, *AIAA Journal* **20**, 88.

Kasting, J. F.: 1982, *J. Geophys. Res.* **87**, 3091.

Kasting, J. F. and Walker, J. C. G.: 1981, *J. Geophys. Res.* **86**, 1147.

Khalil, M. A. K. and Rasmussen, R. A.: 1983. *Tellus* **35B**, 161.

Kuhn, W. R. and Atreya, S. K.: 1979, *Icarus* **37**, 207.

Levine, J. S.: 1982, *J. Molec. Evol.* **18**, 161.

Levine, J. S. and Allario, F.: 1982, *Environ. Monitor. Assess.* **1**, 263.

Levine, J. S. and Boughner, R. E.: 1979, *Icarus* **39**, 310.

Levine, J. S., Augustsson, T. R., and Hoell, J. M.: 1980, *Geophys. Res. Lett.* **7**, 317.

Logan, J. A., Prather, M. J., Wofsy, S. C., and McElroy, M. B.: 1981, *J. Geophys. Res.* **86**, 7210.

Ponnamperuma (ed.), *Comets and the Origin of Life*, D. Reidel, Dordrecht, Holland, pp. 161–190.

Levine, J. S., Augustsson, T. R., and Hoell, J. M.: 1980, *Geophys. Res. Lett.* **7**, p. 317.

Logan, J. A., Prather, M. J., Wofsy, S. C., and McElroy, M. B.: 1981, *J. Geophys. Res.* **86**, 7210.

Lovelock, J. E. and Margulis, L.: 1974, *Tellus* **26**, 1.

Margulis, L. and Lovelock, J. E.: 1974, *Icarus* **21**, 471.

Margulis, L. and Lovelock, J. E.: 1978, *Pure Appl. Geophys.* **16**, 239.

McElroy, M. B., Wofsy, S. C., Penner, J. E., and McConnell, J. C.: 1974, *J. Atmos. Sci.* **31**, 287.

McElroy, M. B., Wofsy, S. C., and Sze, N. D.: 1980, *Atmos. Environ.* **14**, 159.

Oró, J.: 1961, *Nature* **190**, 389.

Rasmussen, R. A. and Khalil, M. A. K.: 1981, *J. Geophys. Res.* **86**, 9826.

Rundel, D. R.: 1977, *J. Atmos. Sci.* **34**, 639.

Walker, J. C. G.: 1977, *Evolution of the Atmosphere*, Macmillan, New York, 318 pp.

Wang, W. C., Yung, Y. L., Lacis, A. A., Mo, T., and Hansen, J. E.: 1976, *Science* **194**, 685.

Weiss, R. F.: 1981, *J. Geophys. Res.* **86**, 7185.